PII S0016-7037(00)00385-9

Stability of layered Ni hydroxide surface precipitates—A dissolution kinetics study

Kirk G. Scheckel,* Andreas C. Scheinost, Robert G. Ford, and Donald L. Sparks

University of Delaware, Department of Plant and Soil Sciences, 140 Townsend Hall, Newark, DE 19717-1303 USA

Abstract—In recent years, studies have shown that sorption of metals onto natural materials results in the formation of new mineral-like precipitate phases. However, the stability of the precipitates and the potential long-term release of the metal back into the soil solution are poorly understood. Therefore, we investigated the influence of residence time and dissolution agent on the release of nickel from three sorbents, pyrophyllite, talc, and gibbsite, complementing the macroscopic observations with X-ray absorption fine structure (XAFS) and diffuse reflectance spectroscopies (DRS), and high-resolution thermogravimetric analysis (HRTGA). Dissolution of the surface precipitates was compared to dissolution of reference Ni compounds.

In the sorption experiments conducted at pH 7.5, Ni-Al layered double hydroxide (LDH) formed in the presence of pyrophyllite and gibbsite, and α-Ni hydroxide formed with talc, in line with former studies. The stability of the phases decreased from Ni-Al LDH on pyrophyllite to α-Ni hydroxide on talc to Ni-Al LDH on gibbsite. This sequence could be explained by the greater stability of precipitates with Al-for-Ni substituted hydroxide layers compared to pure Ni hydroxide layers, and by the greater stability of precipitates with silicate-for-nitrate exchanged interlayer. With increasing residence time, all precipitate phases drastically increased in stability, as was documented by decreasing amounts of Ni released by nitric acid (HNO_3) and ethylenediaminetetraacetic acid (EDTA) treatments. This aging effect may be partly explained by the silicate-for-nitrate exchange during the first days of reaction, and subsequently by silicate polymerization and partial grafting onto the hydroxide layers (Ford et al., 1999). However, even Si-free, Ni-reacted gibbsite showed a substantial aging effect, suggesting that factors other than interlayer silication may be equally important. Such a factor may be crystal growth due to Ostwald ripening. The Ni precipitates which remained at the end of the dissolution experiments were structurally similar to the precipitates at the beginning of the dissolution, indicating that no preferential dissolution of a less stable phase occurred. Therefore, the precipitate phase within each sorbent system was apparently homogeneous in structure. *Copyright © 2000 Elsevier Science Ltd*

1. INTRODUCTION

Sorption reactions at the mineral/water interface largely determine the mobility and bioavailability of metals in soils and sediments. Spectroscopic and microscopic studies in the last decade showed the importance of metal hydroxide precipitate formation upon reacting a variety of clay mineral and oxide surfaces with Ni or Co (Chisholm-Brause et al., 1990; O'Day et al., 1994a; Scheidegger et al., 1996; Towle et al., 1997; Thompson, 1998; Thompson et al., 1999a). In spite of the difficulties studying trace amounts of low-crystalline surface precipitates, substantial advances have been achieved in characterizing their chemical composition and structure. In the case where the sorbent phase released Al during reaction with the metal solutions, the precipitates were predominantly Al-containing layered double hydroxide (LDH) phases (d'Espinose de la Caillerie et al., 1995; Scheidegger et al., 1996; Scheidegger et al., 1997; Scheidegger and Sparks, 1996; Scheidegger et al., 1998; Scheinost et al., 1999; Towle et al., 1997; Thompson, 1998; Thompson et al., 1999a). In the case of Al-free or inert sorbents, however, metal sorption resulted in α-type metal hydroxide precipitates (O'Day et al., 1996; Scheinost et al., 1999; Scheinost and Sparks, 2000). Both types of precipitate consist of brucite-like metal hydroxide layers. In contrast to the well-crystalline hydroxide minerals, however, the layers are separated from each other by water and anions, leading to a turbostratic structure, and metal-metal distances within the layer are significantly reduced with respect to the well-crystalline metal hydroxides (Bish, 1980; d'Espinose de la Caillerie et al., 1995; Génin et al., 1991; Kamath and Therese, 1997; Pandya et al., 1990; Taylor and McKenzie, 1980).

Formation of these precipitate phases drastically reduces metal concentration in soil and sediment solutions, and effectively competes with adsorption onto soil minerals (Elzinga and Sparks, 1999). However, only a few investigations exist trying to assess the stability of these surface precipitates. Scheidegger and Sparks (1996) examined the dissolution of Ni-Al LDH precipitates formed on pyrophyllite using HNO_3 at pH 4 and 6. Nickel detachment was initially rapid at both pH values (with <10% of total Ni released) and was attributable to desorption of specifically adsorbed, mononuclear Ni. Dissolution then slowed down due to the gradual dissolution of the precipitates. In comparison with a β-Ni(OH)$_2$ reference compound the Ni-Al LDH surface precipitates were much more stable. Thompson et al. (1999b) established solubility constants for Co-Al LDH and found also that the Al-containing phase is less soluble than Co hydroxide and Co carbonate at circum-neutral pH. Ford et al. (1999) investigated the dissolution of Ni-Al LDH surface precipitates on pyrophyllite using an EDTA solution at pH 7.5. Detachable Ni drastically decreased when the age of the precipitate increased from 1 h to 1 yr. By employing high-resolution thermogravimetric analysis which is sensitive

---

*Author to whom correspondence should be addressed (scheckel@udel.edu).

to changes in the interlayer composition of LDH, and by paralleling the results of the surface precipitates with those of reference compounds, the authors could show that a substantial part of the aging effect was due to replacement of interlayer nitrate by silicate which transformed the initial Ni-Al LDH into a Ni-Al phyllosilicate precursor. The source of the silicate was the dissolving surface of the pyrophyllite.

These investigations reveal a substantial influence of the sorbent phase on the composition of the precipitate phases and, in turn, on their resistance against dissolution. The objective of this study was to systematically investigate the influence of Al-for-Ni substitution and of silicate-for-nitrate substitution on the kinetics of Ni release. The following sorbents were used:

1. gibbsite to assess the role of Al;
2. talc to assess the role of Si; and
3. pyrophyllite to assess the combined role of Al and Si.

The surface precipitates were subjected to variable residence time periods up to 1 yr before conducting the dissolution experiments in order to study the influence of aging. For comparison, we examined the dissolution of synthesized homogeneous reference phases to reproduce the effect of Al in the hydroxide layer and of exchanged Si in the interlayer. We used two different dissolution agents, EDTA and HNO_3, to compare Ni release by complexation versus release by Ni protolysis (Bryce and Clark, 1996; Stumm, 1997). In addition to describing the dissolution rates macroscopically, we monitored the structure and composition of the remaining Ni phase of the 1-month aged samples using XAFS, DRS, and HRTGA.

2. MATERIALS AND METHODS

2.1. Materials

The pyrophyllite (Robbins, NC, USA; Ward's), talc (Cherokee Co., NC, USA; Excalibur) and gibbsite (Arkansas, USA; Ward's) samples from natural clay deposits were prepared by grinding the clay in a ceramic ball mill for approximately 14 d, centrifuging to collect the <2 μm fraction in the supernatant, Na^+ saturating the <2 μm fraction, and then removing excess salts by dialysis followed by freeze drying of the clay. X-ray diffraction (XRD) showed minor impurities of kaolinite and quartz in pyrophyllite, and about 10% bayerite in the gibbsite. Although the talc sample had about 20% chlorite according to XRD, acid digestion resulted in an Al/Mg ratio of only 0.01. This small Al-content was not sufficient in former experiments to induce the formation of detectable amounts of Ni-Al LDH (Scheinost et al., 1999). The N_2-BET surface areas of the sorbent phases were 95 m^2 g^{-1} for pyrophyllite, 75 m^2 g^{-1} for talc, and 25 m^2 g^{-1} for gibbsite.

The dissolution agents employed in this study were nitric acid (HNO_3) at pH 4 to induce proton-promoted dissolution and 1 mM ethylenediaminetetraacetic acid (EDTA) at pH 7.5 to induce ligand-promoted dissolution. EDTA forms a stable Ni solution complex, and previous studies have shown that EDTA promotes desorption of Ni sorbed to oxide surfaces and the dissolution of poorly crystalline oxide phases (Borggaard, 1992; Bryce and Clark, 1996).

2.2. Ni Sorption and Kinetics of Dissolution

To investigate the influence of aging on the stability of the precipitate phases, pyrophyllite, gibbsite and talc were reacted with Ni for periods of one hour to one year. Experimental conditions were as described in Scheidegger and Sparks (1996) using an initial concentration of 3 mM Ni as $Ni(NO_3)_2$, 10 g/L sorbent and a background electrolyte of 0.1 M $NaNO_3$ at pH 7.5. The systems were purged with N_2 to eliminate CO_2, and the pH was maintained through addition of 0.1 M NaOH via a Radiometer pH-stat titrator. After one week, the

Table 1. Ni sorption (mol kg^{-1}) on pyrophyllite, talc and gibbsite for various reaction aging times correlating to the dissolution experiments.

Time	Pyrophyllite	Talc	Gibbsite
1 hr	0.12	0.10	xx
12 hr	0.23	0.20	xx
24 hr	0.27	0.25	0.06
3 d	xx	xx	0.16
7 d	xx	xx	0.21
1 mon	0.30	0.30	0.28
3 mon	0.30	0.30	0.29
6 mon	0.30	0.30	0.30
1 yr	0.30	0.30	0.30

batch reaction vessel was sealed and placed in a 25°C incubation chamber. At weekly intervals, the suspension pH was readjusted to 7.5 while purging with N_2. Sorption levels at the various aging times are shown in Table 1.

Dissolution was carried out by a replenishment technique using 1 mM EDTA at pH 7.5 or HNO_3 at pH 4.0. From the aging Ni/clay mineral suspensions, 30 mL (corresponding to 300 mg of clay) were withdrawn. After centrifuging at 17,000 rpm for 5 minutes, the supernatant was decanted, and 30 mL of the dissolution agent was added to the remaining solids. The suspensions were then placed on a reciprocating shaker at 25°C for 24 h. The extraction steps were repeated either 10 times (= 10 days) for short-term (aged <1 month) or 14 days for long-term (aged >1 month) Ni sorption samples. ICP-AES or AAS was used to determine Ni and Si in the supernatants during dissolution.

A disadvantage of the replenishment technique is that there will inevitably be some dissolved Ni entrained in the clay paste and one could argue the formation of Ni-EDTA complexes on the surfaces. However, this accounts for a very small percentage of the overall Ni released. This is supported by the fact that the rate of dissociation for the Ni-EDTA complexes is slow relative to the residence time of the complexes in solution before replenishment (van den Berg and Nimmo, 1987; Hering and Morel, 1990; Wilkens, 1974). The conditional stability constant (K^{cond}) for Ni-EDTA complexes is approximately 10^{10} M^{-1}. Sorption of Ni-EDTA complexes is also unlikely under the reaction conditions of this study (Nowack and Sigg, 1996; Elliot and Huang, 1979; Elliot and Denneny, 1982; Chang and Ku, 1994) suggesting the complexes prefer to remain in solution once formed. Additionally, the maximum solution concentration of Ni after any given 24 h replenishment period was 0.46 mM which is far below the saturation point for re-precipitation of Ni under these reaction conditions either on the sorbent or in bulk solution, especially during dissolution with HNO_3 at pH 4.0.

2.3. Synthesis of Ni Reference Compounds

An α-Ni hydroxide was prepared by adding 550 mL of 30% ammonia to 500 mL of 1 M $Ni(NO_3)_2$ (Génin et al., 1991). The solution was vigorously stirred and purged with N_2. After 2 h, the suspension was centrifuged and washed with D.I. water in five cycles, shock-frozen in liquid N_2, and freeze-dried. A Ni-Al LDH sample was prepared by controlled hydrolysis (Taylor, 1984). The amount of Ni and Al (added as $Ni(NO_3)_2 \cdot 9H_2O$ and $Al(NO_3)_3 \cdot 9H_2O$) was adjusted to give an initial Ni/Al ratio in solution of 10. Under vigorous stirring, 450 mL of both solutions were combined. The pH was raised to 6.9 by addition of 2.5 M NaOH and then kept constant for 5 h using an autotitrator. The precipitate was washed and dried as before. Metal solutions were purged with N_2, and the 2.5 M NaOH was freshly prepared to minimize carbonate uptake by the precipitate. By acid digestion a Ni/Al ratio of 5 was determined. XRD-layer spacings and strong nitrate bands in the IR spectra of the α-Ni hydroxide and the Ni-Al LDH samples confirmed the prevalence of nitrate in the interlayer. Part of both samples was subsequently exchanged with silicate following the method of Depège et al. (1996) 100 mL deionized-distilled H_2O + 0.85 g sodium metasilicate + 0.4 g Ni-Al hydrotalcite, giving a pH of 12.2. The suspensions were heated at 90°C for 24 h under an N_2 atmosphere, and subsequently aged 2 weeks at 60°C in a sealed vessel (final pH = 12.0).

The silicate-for-nitrate exchange was confirmed by FTIR. Further data on these samples are given by Scheinost et al. (1999) and Scheinost and Sparks (2000).

2.4. Spectroscopic and Thermogravimetric Characterization of Surface Precipitates

Changes in the solid phase Ni speciation during dissolution were periodically assessed via spectroscopic and thermoanalytical techniques. For XAFS and DRS analyses, samples were examined in-situ by centrifuging the suspensions and using the wet clay paste. For HRTGA analyses, the clay pastes were washed three times with D.I. water and freeze-dried before examination. Speciation of dissolution samples was carried out for clay samples aged for 1 month to ensure that only a negligible part of the Ni was bound as an adsorption complex, while the majority was present as a surface precipitate.

XAFS was applied to determine information on the nearest-neighbor chemical environment of Ni such as coordination numbers and atomic distances. Experiments were conducted at the National Synchrotron Light Source (NSLS), Brookhaven National Laboratory (BNL), Upton, New York, on beamline X-11A. The electron storage ring was operated at 2.528 GeV with beam currents in the 180–310 mA range. A 0.5 mm premonochromator slit width and a Si(111) double-crystal monochromator detuned by 25% to reject higher-order harmonics was used. The beam energy was calibrated by assigning the first inflection of the K_α-absorption edge of nickel metal to 8333 eV. The XAFS spectra were collected in fluorescence mode using a Lytle detector. The ionization chamber of the Lytle detector was filled with Ar and the chamber of I_o was filled with N_2 gas. Samples were positioned at a 45° angle relative to the incident beam and the ionization chamber was situated at 45° off the sample (90° off the incident beam). A Co-3 filter and Soller slits were arranged between the sample and the Lytle detector to reduce scattered X-rays reaching the fluorescence detector. Spectra were collected at 77 K to reduce thermal disorder. Previous studies in our laboratory indicate that Ni speciation does not change by cooling to 77 K versus room temperature (Roberts et al., 1999). Triplicate scans were collected for each sample.

MacXAFS 4.0 (Bouldin et al., 1995) was employed for background subtraction and Fourier filtering. The χ function was extracted from the raw data by using a linear preedge background and a spline postedge background, and by normalizing the edge to unity. The data were next converted from energy to k space and weighted by k^3 to compensate for the dampening of the XAFS amplitude with increasing k. Structural parameters were extracted with fits to the standard XAFS equation. Using the FEFF6 and ATOMS codes (Zabinsky et al., 1995), ab initio amplitude and phase functions for single shells were calculated. A natural takovite ($Ni_6Al_2(OH)_{16}CO_3 \cdot H_2O$) (Kambalda W. A., Australia) and a synthetic β-Ni(OH)$_2$ (Johnson Mattey Co.) were used as reference compounds. Multishell fitting was done in R space over the range $1.104 < R < 3.129$ Å with $3.2 < k < 13.6$ Å^{-1} for pyrophyllite and gibbsite samples and $1.104 < R < 3.191$ Å with $3.2 < k < 13.6$ Å^{-1} for talc samples. The number of free floating parameters was reduced by one by allowing only equal values for the Debye-Waller factors of the Ni-Ni and Ni-Al shells. The R_{Ni-O} and R_{Ni-Ni} values are estimated to be accurate to ± 0.02 Å, and the N_{Ni-O} and N_{Ni-Ni} are estimated to be accurate to $\pm 20\%$. The estimated accuracies for N_{Ni-Al} and R_{Ni-Al} are $\pm 60\%$ and ± 0.06 Å, respectively. The accuracy estimates are based on the results of theoretical fits to spectra of the reference compounds of known structure (O'Day et al., 1994b).

Although the information provided by DRS is restricted to local symmetry of the first coordination shell, it is more sensitive to changes in the coordination distance of Ni-O (R_{Ni-O}) than XAFS. Therefore, this method proved to be very sensitive in distinguishing between Ni-Al LDH (smaller R_{Ni-O}) and α-Ni hydroxide (larger R_{Ni-O}) by using the energy position of the $\nu 2$ band which corresponds to the $^3A_{2g} \rightarrow \, ^3T_{1g}$ transition (Scheinost et al., 1999). A Perkin Elmer Lambda 9 diffuse reflectance spectrophotometer fitted with a 5 cm Spectralon-coated integrating sphere was employed to collect spectra in the UV-VIS-NIR range. Extraction of the band position is described in Scheinost et al. (1999).

HRTGA was employed to characterize thermal decomposition reactions attributed to the Ni precipitate phases in the reacted clay mineral samples. Changes in the quantity and temperature of decomposition are indicative of compositional changes in the precipitate. We employed a TA Instruments 2950 High-Resolution Thermogravimetric analyzer to examine approximately 15–20 mg samples from sorption and dissolution studies that were previously freeze-dried. The analysis was run under a N_2 atmosphere over a temperature range of 30 to 800°C. The following high-resolution settings were used:

1. maximum heating rate = 20°C min^{-1};
2. resolution = 5.0; and
3. sensitivity = 1.0 (Ford and Bertsch, 1999).

Data are presented as the derivative of the weight loss curve versus temperature.

3. RESULTS

3.1. Macroscopic Dissolution Data

The macroscopic dissolution data are assembled in Figure 1 and are presented as the relative amount of Ni remaining on the surfaces. For all clay minerals and both dissolution agents, the fraction of extracted Ni decreased as the age of the Ni complexes increased from 1 h to 1 yr. As shown in Figure 2 for samples aged 1 month, ligand-promoted dissolution by EDTA was more effective than the protolysis by HNO$_3$ at pH 4. At this aging time, extraction with EDTA indicated the following order of increasing Ni stability for the sorbent systems, gibbsite < talc < pyrophyllite. However, extraction at pH 4 with HNO$_3$ indicated the following order, talc < gibbsite < pyrophyllite. This behavior appears to depend primarily on the extractant, since after aging for a year the stability of sorbed Ni is consistent with results established using EDTA at 1 month aging (Fig. 3). The results shown in Figure 3 are based on the percentage of unextracted Ni following 10 replenishments of the dissolution agent. The most dramatic increase in the stability of sorbed Ni occurs within the first 50 d for all aging systems. These macroscopic results suggest that the elemental composition of the sorbent played a role in determining the long-term stability of sorbed Ni.

3.2. XAFS of Dissolution Samples

XAFS spectra were collected for pyrophyllite and talc reacted with Ni for 1 month, and subsequently subjected to dissolution by EDTA for 1 to 7 d (Fig. 4). The k^3-weighted χ functions of pyrophyllite (Fig. 4a) show a beat pattern at 8 Å^{-1} which is characteristic for Ni-Al LDH (Scheinost and Sparks, 2000). This pattern remains unchanged after all dissolution steps, indicating that the initial phase, the dissolved phase and the remaining phase consist predominantly of Ni-Al LDH with about the same Ni/Al ratio. This result is further confirmed by XAFS fits to the radial structure functions (RSFs) (Fig. 4c,d). The fit data show that Ni is surrounded by 6 O atoms at an average distance of 2.05 Å, by 5 Ni atoms at 3.06 Å, and by 1–2 Al atoms at 3.11 Å (Table 2). These local structural data are consistent with those of Ni-Al LDH (Scheidegger et al., 1998; Scheinost and Sparks, 2000), and do not indicate any change with increasing dissolution. The fit data for Ni-reacted talc (Fig 4d) show that Ni is surrounded by 6 Ni atoms at 3.08 Å, which is consistent with α-Ni hydroxide (Pandya et al., 1990; Scheinost and Sparks, 2000). The lack of the characteristic beat pattern at 8 Å^{-1} in the corresponding χ functions confirms the
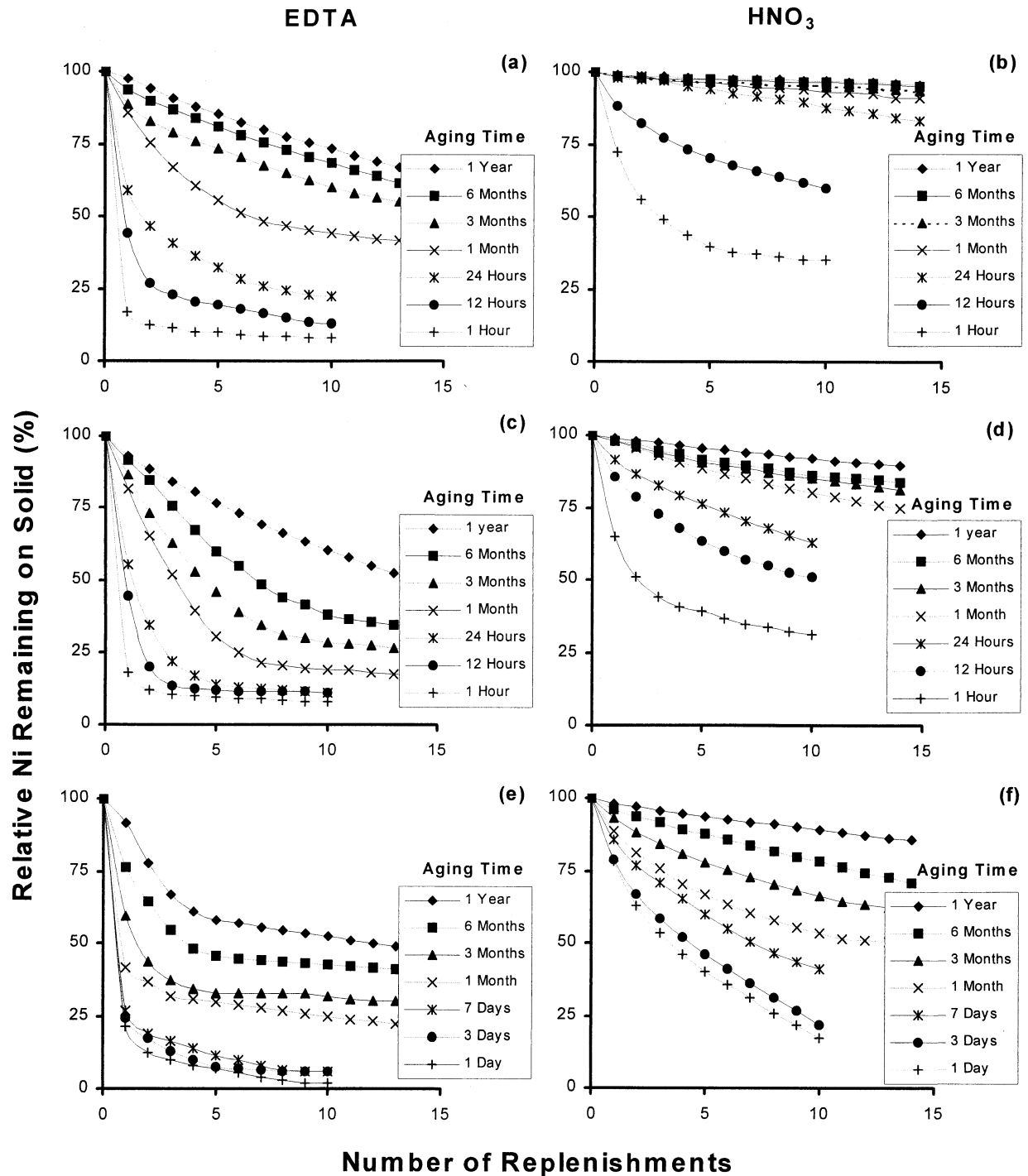
EDTA **HNO₃**

Fig. 1. Rate of Ni removal from Ni-reacted clay minerals as a function of aging of the surface precipitates. Replenishment steps with EDTA at pH 7.5 are shown on the left side, and replenishment steps with HNO₃ at pH 4.0 on the right side. Ni-reacted clay minerals are from top: pyrophyllite (a & b), talc (c & d), and gibbsite (e & f).

conclusions from the fit (Fig 4b). Again, the initial precipitate, the dissolved phase, and the remaining precipitate have an identical local structure. Treatment with HNO_3 also did not show any change of the initial precipitate phase with progressing dissolution (not shown).

3.3. DRS of Dissolution Samples

The crystal field splitting of Ni^{2+} in an octahedral O cage is very sensitive to small changes in Ni-O bond distances (Burns, 1993). Therefore, DRS can be used to distinguish between
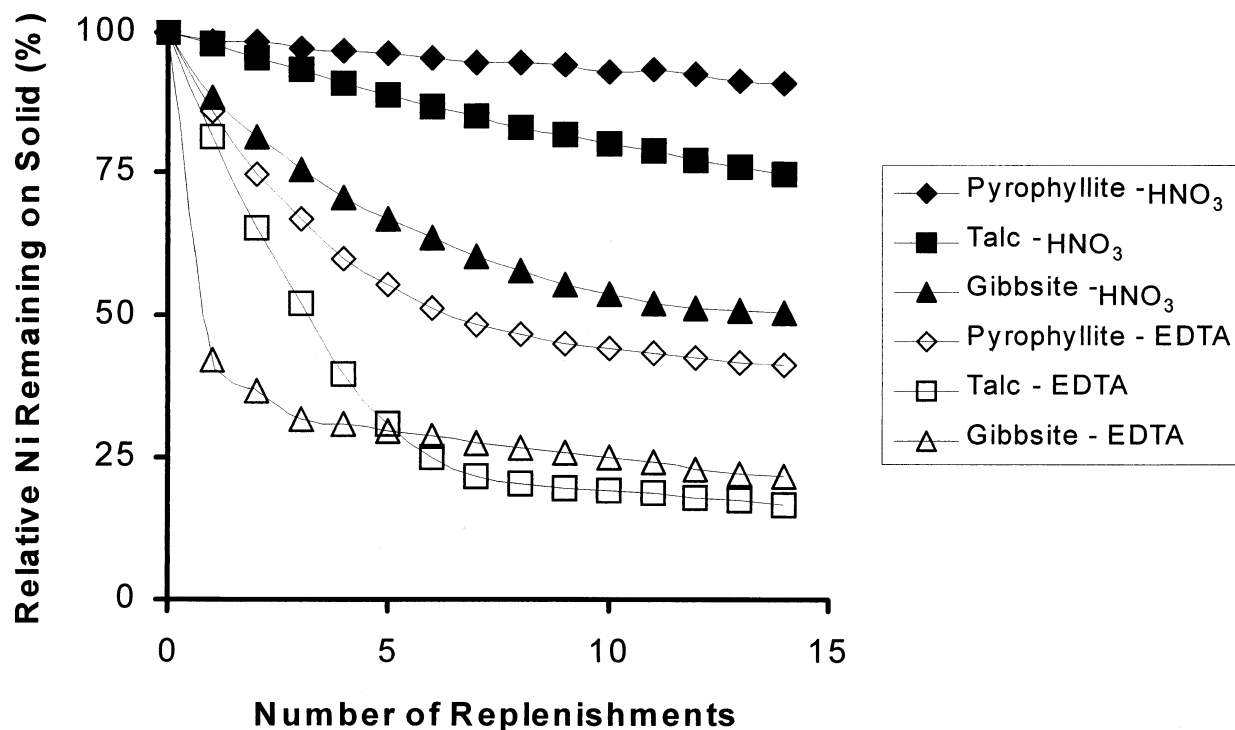
Fig. 2. Rate of Ni removal from Ni-reacted clay minerals as a function of sorbent identity and dissolution treatment. Ni-reacted clay minerals have been aged for 1 month prior to dissolution (extract of Fig. 1).

Ni-Al LDH and α-Ni hydroxide (Scheinost et al., 1999). Consistent with the XAFS results shown before, the $\nu 2$ band position of 15,300 cm^{-1} for pyrophyllite (Fig. 5a) and gibbsite (Fig. 5b) indicates Ni-Al LDH, and the $\nu 2$ band position of 14,900 cm^{-1} for talc (Fig 5c) indicates α-Ni hydroxide. In all cases, band positions do not change with increasing dissolution. Because the absorption coefficient of a mononuclear Ni^{2+} adsorption complex is 2 orders of magnitude lower than that of Ni^{2+} in a three-dimensional, polynuclear structure, band heights are indicative of the amount of Ni present in a precipitate phase (Scheinost et al., 1999). Therefore, the decrease of band heights with increasing Ni removal (Fig. 5) is clear evidence that the removed Ni is predominantly due to dissolution of the precipitate phase and not due to desorption of adsorbed Ni.

3.4. HRTGA of Dissolution Samples

High-resolution thermogravimetric analysis (HRTGA) was successfully employed to show that a Ni-Al LDH precipitate on pyrophyllite transforms into a Ni-Al phyllosilicate precursor within 1 yr at ambient temperature and pressure (Ford et al., 1999). This transformation progresses by silicate-for-nitrate exchange in the interlayer, and the subsequent polymerization of single silicate units which may then become connected with the octahedral hydroxide layers (Depège et al., 1996). This transformation is not detectable by DRS or XAFS (Ford et al., 1999; Scheinost et al., 1999; Scheinost and Sparks, 2000). Therefore, we employed HRTGA to investigate if a similar

transformation has occurred during the 1 month aging time on pyrophyllite, and whether detectable changes of the interlayer composition occur during dissolution. The derivatives of the weight loss curves (Fig. 6) show a maximum at about 280°C which is due to dehydroxylation of the octahedral layer and the complete collapse of the LDH structure (Bellotto et al., 1996; Ford et al., 1999). However, no weight loss at 220°C is detectable which would occur due to water and nitrate expulsion (Bellotto et al., 1996; Ford et al., 1999). This indicates that nitrate has been exchanged by silicate in the Ni-Al LDH interlayer. No change occurs with sequential dissolution steps. Therefore, not only the local structure within the octahedral Ni hydroxide layer remains constant with dissolution (XAFS, DRS), but also the interlayer composition.

4. DISCUSSION

Former DRS work has shown that detectable amounts of Ni precipitates formed within 5 min. on pyrophyllite, 7 h on talc, and 24 h on gibbsite under similar experimental conditions (Scheinost et al., 1999). For aging times up to one year, the precipitate phase was a Ni-Al LDH on pyrophyllite and an α-Ni hydroxide on talc (Scheidegger and Sparks, 1996; Scheinost et al., 1999). For gibbsite, the initial precipitate phase after 24 h was prevalently an α-Ni hydroxide which transformed into a Ni-Al LDH with aging (Scheinost et al., 1999). Our DRS and XAFS results on sorbed samples (not shown) are fully consistent with these former results. In all systems, some of the Ni sorbed onto the clay mineral surfaces may have been present as
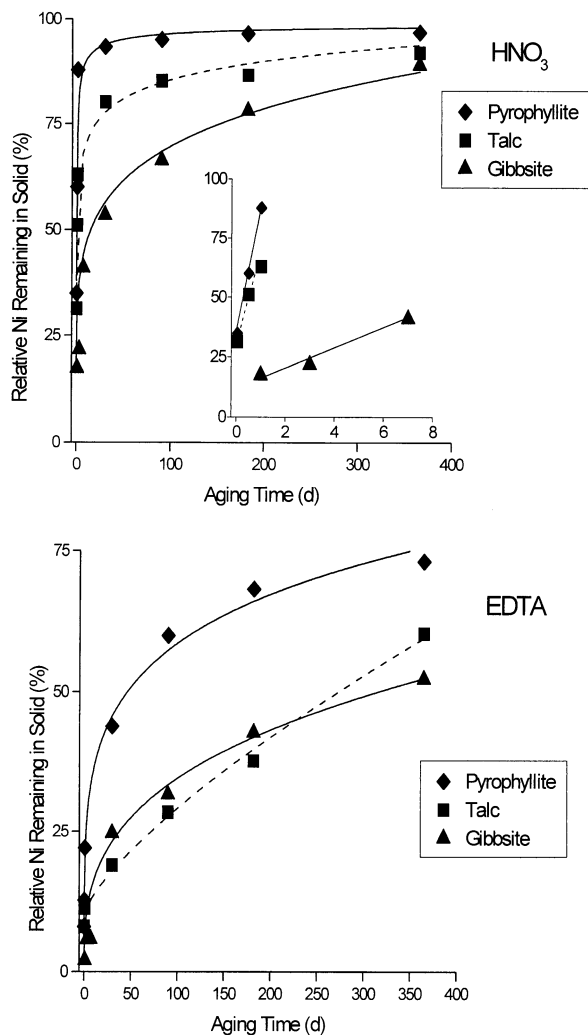
Fig. 3. Ni remaining on solids after 10 replenishment steps as a function of aging of the Ni-reacted clay minerals (extract of Fig. 1). The inset of 3a shows the early aging times.

adsorbed Ni. However, this adsorbed Ni constitutes a small fraction of the overall Ni in the system after one-day reaction time (Scheidegger et al., 1997; Scheidegger et al., 1998; Scheinost et al., 1999). Therefore, removal of Ni from the clay minerals aged for at least 1 d is prevalently due to dissolution of the two different precipitate phases. This is further substantiated by the decrease of the $\nu 2$ band height with sequential dissolution steps (Fig. 5).

As can be derived from Figure 3, the Ni-Al LDH surface precipitate on pyrophyllite was more resistant to dissolution by HNO$_3$ and EDTA than the α-Ni hydroxide phase on talc and the Ni-Al LDH phase on gibbsite. Former work has suggested that Al-containing Ni or Co hydroxides are more resistant to dissolution than the pure metal hydroxides (Scheidegger and Sparks, 1996; Thompson et al., 1999b). However, only part of the observed stability sequence can be explained by this difference between Ni-Al LDH and α-Ni hydroxide. Therefore, the stability of the surface precipitates was determined by more factors than the Al-for-Ni substitution in the hy-

droxide layers alone. The work by Ford et al. (1999) showed that the stability of a Ni-Al LDH surface precipitate on pyrophyllite was drastically enhanced by exchange of interlayer nitrate by polymerizing silicate. The source of the silicate was the dissolution of the pyrophyllite surface during sorption of Ni. Hence, the higher stability of the pyrophyllite Ni-Al LDH may be explained by silication, and the smaller stability of gibbsite Ni-Al LDH by the lack of structural Si. The lack of the 220°C weight loss event that is attributed to interlayer nitrate in the HRTGA weight loss curves of Ni-pyrophyllite indeed supports the silication hypothesis (Fig. 6). Since the Ni hydroxide layers of α-Ni hydroxide forming under our experimental conditions should also be separated by water and nitrate (Génin et al., 1991; Scheinost and Sparks, 2000), a similar silicate-for-nitrate exchange may occur with the surface precipitate on talc, explaining its greater stability compared to the gibbsite Ni-Al LDH (Fig. 3).

To further substantiate the influence of interlayer silication on the dissolution stability of Ni-Al LDH and α-Ni hydroxide, we investigated the dissolution kinetics of reference compounds where the interlayer composition was verified by FTIR spectroscopy (Fig. 7). Using HNO$_3$ at pH 4.0, α-Ni hydroxide dissolved more rapidly than Ni-Al LDH, in line with the results by Scheidegger et al. (1996) and Thompson et al. (1999b). However, Si-exchange of both layered hydroxide phases drastically increased their stability. Note that the Si-exchanged α-Ni hydroxide is even more stable than the original Ni-Al LDH. The observed ranking of the reference compound stabilities strongly supports the contention that the lower stability of Ni-gibbsite is due to nitrate Ni-Al LDH, while both the α-Ni hydroxide on talc and the Ni-Al LDH on pyrophyllite have silicated interlayers. Therefore, the observed ranking of surface precipitate stabilities (Fig. 3) can be explained by a combination of Al-for-Ni substitution within the hydroxide layers and silicate-for-nitrate substitution in the interlayers.

Consequently, the increasing stability of the surface precipitates on talc and pyrophyllite with time (Fig. 3) can be explained by the silicate-for-nitrate exchange within the first days, and the subsequent silicate polymerization and partial grafting onto the hydroxide layers, in line with the results of Depège et al. (1996) and Ford et al. (1999). However, the LDH phase on gibbsite shows a substantial stabilization against dissolution with aging, too (Fig. 3). Thus, another factor besides silication must be responsible for this aging effect. This factor could be crystal growth due to Ostwald ripening, which could also lead to decrease of dissolution kinetics (Sutheimer et al., 1999). Furthermore, it cannot be excluded that crystal growth may also be responsible for a substantial part of the aging of surface precipitates on talc and pyrophyllite. We are currently employing high-resolution transmission electron microscopy (HRTEM) to quantify a possible crystal growth of the surface precipitates with time.

Three techniques, XAFS, DRS and HRTGA, were employed to monitor possible changes in the structure of the surface precipitate of 1 month aged Ni pyrophyllite during dissolution (Figs. 4–6). As no change was observed one could conclude that the precipitate dissolution behavior was analogous to the dissolution of a single phase. That is, we did not find evidence
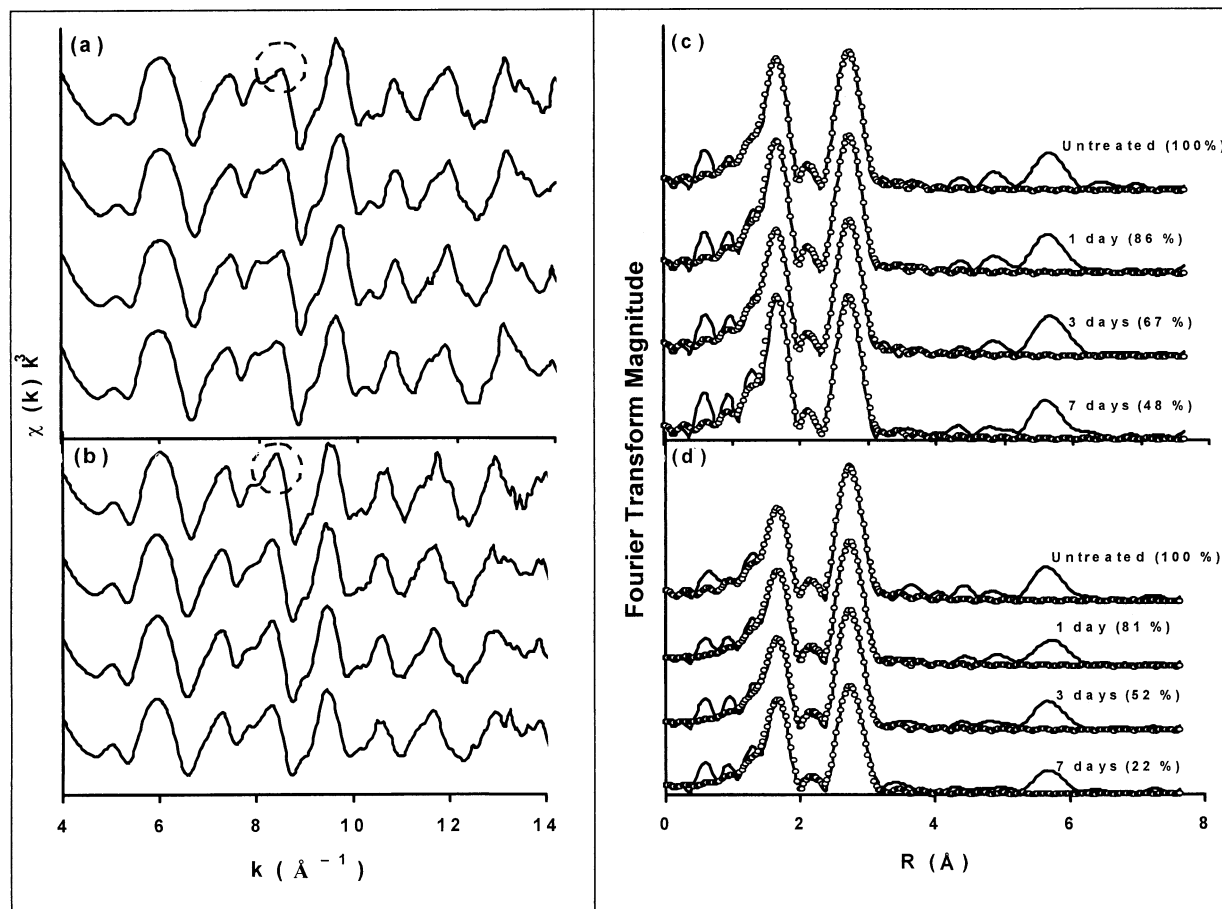
Fig. 4. Ni-K_α XAFS spectra of pyrophyllite (a and c) and talc (b and d) aged with Ni for one month and subsequently treated with EDTA (pH 7.5) for 1, 3, and 7 d. The k^3 weighted χ functions are shown on the left side, and the measured (solid lines) and fitted (dotted lines) radial structure functions are shown on the right side (uncorrected for phase shifts). The circle shows a key identification for Ni-Al LDH versus α-Ni hydroxide (Scheinost and Sparks, 2000).

that the surface precipitate on pyrophyllite consists of a population of crystals of different composition or structure, where

more labile structures would dissolve first and more stable structures would remain.

Table 2. Structural parameters derived from XAFS analysis for dissolution (EDTA pH 7.5) of nickel aged for one month on pyrophyllite and talc.

Sample & dissolution time	ΔE_o (eV)	Ni-O			Ni-Ni			Ni-Al		
		R (Å)[a]	N[b]	σ^2 (Å^2)[c]	R (Å)[a]	N[b]	σ^2 (Å^2)[d]	R (Å)[a]	N[b]	σ^2 (Å^2)[d]
Pyrophyllite										
Untreated	4.7	2.05	6.0	0.003	3.06	4.9	0.003	3.11	1.4	0.003
1 day	3.8	2.05	6.0	0.003	3.06	5.2	0.004	3.12	1.7	0.004
3 day	4.4	2.05	6.0	0.003	3.06	4.9	0.003	3.12	1.2	0.003
7 day	3.9	2.05	6.0	0.002	3.06	5.1	0.003	3.11	1.6	0.003
Talc										
Untreated	3.6	2.05	6.0	0.003	3.08	6.0	0.003			
1 day	2.9	2.05	6.0	0.003	3.08	5.9	0.004			
3 day	3.0	2.05	6.0	0.004	3.08	6.0	0.005			
7 day	2.7	2.05	6.0	0.003	3.08	5.7	0.005			

[a] Interatomic distance.
[b] Coordination number.
[c] Debye-Waller factor.
[d] Debye-Waller factors for pyrophyllite (Ni-Ni and Ni-Al) were constrained to be equal.
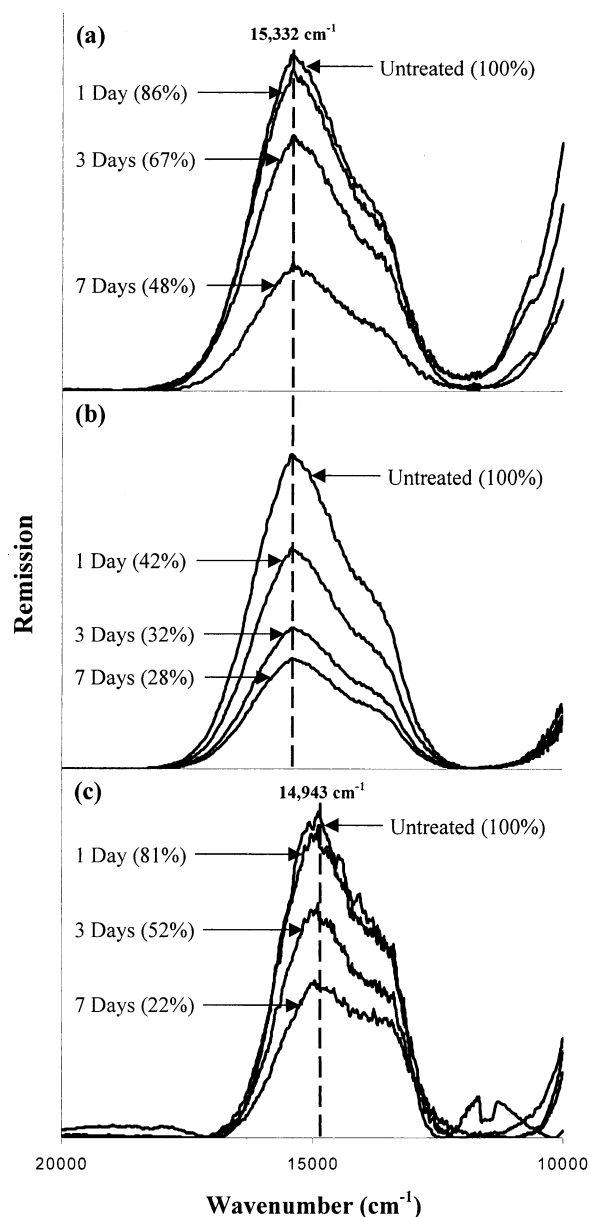
Fig. 5. The DRS $\nu 2$ absorption band for the Ni surface precipitates on (a) pyrophyllite, (b) gibbsite, and (c) talc aged for 1 month ("untreated") and subsequently extracted with EDTA (pH 7.5) for 1, 3, and 7 d. The relative amount of Ni remaining on the clay mineral is also given.

5. CONCLUSIONS

In this study, an array of analytical techniques was applied to examine the dissolution of Ni surface precipitates formed on pyrophyllite, talc, and gibbsite. The differences in stability of the surface precipitates could be explained by a combination of Al-for-Ni substitution in the hydroxide layers and silicate-for-nitrate substitution in the interlayer. The macroscopic dissolution studies demonstrated increased stability in Ni surface precipitates with aging. The aging effect may be attributed partly to the solid-state transformation of the
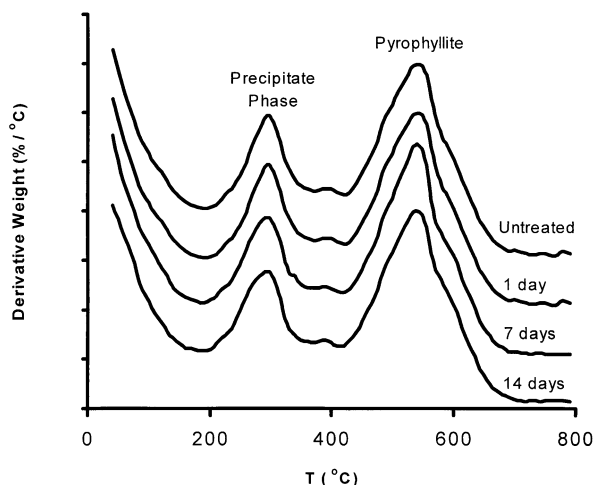

Fig. 6. High-resolution thermogravimetric analysis (HRTGA) of the Ni surface precipitate on pyrophyllite aged for one month ("untreated") following extraction with HNO_3 (pH 4) for 1, 7, and 14 d. The weight loss event at about 280°C is indicative of Ni-Al LDH (Ford et al., 1999), while the weight loss between 450 and 600°C is due to pyrophyllite (Evans and Guggenheim, 1988).

precipitate phases (silication of Ni-Al LDH and α-Ni hydroxide), and partly to crystal growth due to Ostwald ripening.

The ubiquity of metastable Al and Si-containing minerals in soils and sediments makes the formation of Ni-Al LDH and its transformation into a Ni-Al phyllosilicate precursor at circumneutral and basic pH very likely. The formation of a Ni-Al LDH precipitate has been confirmed after reacting soil clay fractions and a whole soil with Ni at pH > 6.8 (Roberts et al., 1999). The formation of Ni surface precipitates, and the effect of aging on these precipitates, may drastically reduce the ecotoxicity of Ni in soils and sediments.
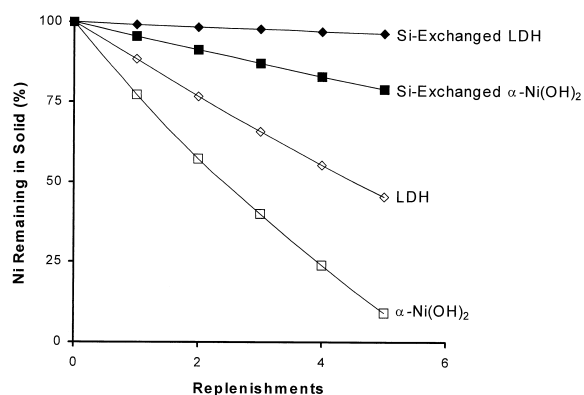
Fig. 7. Ni release by HNO_3 at pH 4.0 from homogeneous synthetic Ni-Al LDH and α-Ni hydroxide, both with either predominantly nitrate or silicate in the interlayer.

REFERENCES

Bellotto M., Rebours B., Clause O., Lynch J., Bazin D., and Elkaim E. (1996) Hydrotalcite decomposition mechanism: A clue to the structure and reactivity of spinel-like mixed oxides. *J. Phy. Chem.* **100,** 8535–8542.

Bish D. L. (1980) Anion-exchange in takovite: Applications to other hydroxide minerals. *Bull. Mineral.* **103,** 170–175.

Borggaard O. K. (1992) Dissolution of poorly crystalline iron oxides in soils by EDTA and oxalate. *Zeitschrift fu̇r Pflanzenernȧhrung und Bodenkunde* **155,** 431–436.

Bouldin C., Elam T., and Furenlid L. (1995) MacXAFS—An EXAFS analysis package for Macintosh. *Physica B* **208/209,** 190–192.

Bryce A. L. and Clark S. B. (1996) Nickel desorption kinetics from hydrous ferric oxide in the presence of EDTA. *Coll. Surf.* **107,** 123–130.

Burns R. G. (1993) Mineralogical Applications of Crystal Field Theory. Cambridge University Press.

Chang C. and Ku Y. (1994) Adsorption-kinetics of cadmium chelates on activated carbon. *J. Haz. Mat.* **38,** 439–451.

Chisholm-Brause C. J., O'Day P. A., Brown G. E., Jr., and Parks G. A. (1990) Evidence for multinuclear metal-ion complexes at solid-solution interfaces from x-ray absorption spectroscopy. *Nature* **348,** 528–530.

Depège C., El Metoui F.-Z., Forano C., de Roy A., Dupuis J., and Besse J.-P. (1996) Polymerization of silicates in layered double hydroxides. *Chem. Mat.* **8,** 952–960.

d'Espinose de la Caillerie J. B., Kermarec M., and Clause O. (1995) Impregnation of γ-alumina with Ni(II) and Co(II) ions at neutral pH: Hydrotalcite-type coprecipitate formation and characterization. *J Am. Chem. Soc.* **117,** 11471–11481.

Elliott H. A. and Huang C. P. (1979) Adsorption characteristics of Cu(II) in the presence of chelating-agents. *J. Coll. Inter. Sci.* **70,** 29–44.

Elliott H. A. and Denneny C.M. (1982) Soil adsorption of cadmium from solutions containing organic-ligands. *J. Env. Qual.* **11,** 658–663.

Elzinga E. J. and Sparks D. L. (1999) Nickel sorption mechanism in a pyrophyllite-montmorillonite mixture. *J. Coll. Inter. Sci.* **213,** 506–512.

Evans B. W. and Guggenheim S. (1988) Talc, pyrophyllite, and related minerals. In *Hydrous Phyllosilicates* (ed. S. W. Bailey). Vol. 19 Mineralogical Society of America.

Ford R. G. and Bertsch P. M. (1999) Distinguishing between surface and bulk dehydration-dehydroxylation reactions in synthetic goethites by high-resolution thermogravimetric analysis. *Clays Clay Min.* **47(3),** 329–337.

Ford R. G., Scheinost A. C., Scheckel K. G., and Sparks D. L. (1999) The link between clay mineral weathering and structural transformation in Ni surface precipitates. *Env. Sci. Tech.* **33(18),** 3140–3144.

Génin P., Delahaye-Vidal A., Portemer F., Tekaia-Elhsissen K., and Figlarz M. (1991) Preparation and characterization of α-type nickel hydroxides obtained by chemical precipitation: Study of the anionic species. *Eur. J. Solid State Inorg. Chem.* **28,** 505–518.

Hering J. G. and Morel F. M. M. (1990) Kinetics of trace-metal complexation–ligand–exchange reactions. *Env. Sci. Tech.* **24,** 242–252.

Kamath P. V. and Therese G. H. A. (1997) On the existence of hydrotalcite-like phases in the absence of trivalent cations. *J. Solid State Chem.* **128,** 38–41.

Nowack B. and Sigg L. J. (1996) Adsorption of EDTA and metal-EDTA complexes onto goethite. *J. Coll. Inter. Sci.* **177,** 106–121.

O'Day P. A., Brown G. E., and Parks G. A. (1994a) X-ray absorption spectroscopy of cobalt(II) multinuclear surface complexes and surface precipitates on kaolinite. *J. Coll. Inter. Sci.* **165,** 269–289.

O'Day P. A., Rehr J. J., Zabinsky S. I., and Brown Jr. G. E. (1994b) Extended X-ray absorption fine structure (EXAFS) analysis of disorder and multiple-scattering in complex crystalline solids. *J. Am. Chem. Soc.* **116,** 2938–2949.

O'Day P. A., Chisholm-Brause C. J., Towle S. N., Parks G. A., and Brown Jr. G. E. (1996) X-ray absorption spectroscopy of Co(II) sorption complexes on quartz (a-SiO2) and rutile (TiO2). *Geochim. Cosmochim. Acta* **60(14),** 2515–2532.

Pandya K. I., O'Grady W. E., Corrigan D. A., McBreen J., and Hoffman R. W. (1990) Extended x-ray absorption fine structure investigation of nickel hydroxides. *J. Phys. Chem.* **94,** 21–26.

Roberts D. R., Scheidegger A. M., and Sparks D. L. (1999) Kinetics of mixed Ni-Al precipitate formation on a soil clay fraction. *Env. Sci. Tech.* **33,** 3749–3754.

Scheidegger A. M., Fendorf M., and Sparks D. L. (1996) Mechanisms of nickel sorption on pyrophyllite: Macroscopic and microscopic approaches. *Soil Sci. Soc. Am. J.* **60,** 1763–1772.

Scheidegger A. M., Lamble G. M., and Sparks D. L. (1997) Spectroscopic evidence for the formation of mixed-cation hydroxide phases upon metal sorption on clays and aluminum oxide. *J. Coll. Inter. Sci.* **186,** 118–128.

Scheidegger A. M. and Sparks D. L. (1996) Kinetics of the formation and the dissolution of nickel surface precipitates on pyrophyllite. *Chem. Geol.* **132,** 157–164.

Scheidegger A. M., Strawn D. G., Lamble G. M., and Sparks D. L. (1998) The kinetics of mixed Ni-Al hydroxide formation on clays and aluminum oxides: A time-resolved XAFS study. *Geochim. Cosmochim. Acta* **62,** 2233–2245.

Scheinost A. C., Ford R. G., and Sparks D. L. (1999) The role of Al in the formation of secondary Ni precipitates on pyrophyllite, gibbsite, talc, and amorphous silica: A DRS study. *Geochim. Cosmochim. Acta* **63,** 3193–3203.

Scheinost A. C. and Sparks D. L. (2000) Formation of layered single and double metal hydroxide precipitates at the mineral/ water interface: A multiple-scattering XAFS analysis. *J. Coll. Inter. Sci.* **223,** 167–178.

Stumm W. (1997) Reactivity at the mineral-water interface: Dissolution and inhibition. *Coll. Surf. A. Physicochem. Eng. Asp.* **120(1–3),** 143–166.

Sutheimer S. H., Maurice P. A., and Zhou Q. (1999) Dissolution of well and poorly crystallized kaolinites: Al speciation and effects of surface characteristics. *Am. Mineral.* **84,** 620–628.

Taylor R. M. (1984) The rapid formation of crystalline double hydroxy salts and other compounds by controlled hydrolysis. *Clay Minerals* **19,** 591–603.

Taylor R. M. and McKenzie R. M. (1980) The influence of aluminum on iron oxides. VI. The formation of Fe(II)-Al(III) hydroxy-chlorides, -sulfates, and -carbonates as new members of the pyroaurite group and their significance in soils. *Clays and Clay Minerals* **28(3),** 179–187.

Thompson H. A. (1998) Dynamic ion partitioning among dissolved, adsorbed, and precipitated phases in aging cobalt(II)/kaolinite/water systems. Ph.D., Stanford University.

Thompson H. A., Parks G. A., and Brown G. E., Jr. (1999a) Dynamic interactions of dissolution, surface adsorption, and precipitation in an aging cobalt(II)-clay-water system. *Geochim. Cosmochim. Acta* **63,** 1767–1779.

Thompson H. A., Parks G. A., and Brown Jr. G. E. (1999b) Ambient-temperature synthesis, evolution, and characterization of cobalt-aluminum hydrotalcite-like solids. *Clays Clay Mineral.* **47,** 425–438.

Towle S. N., Bargar J. R., Brown G. E., and Parks G. A. (1997) Surface precipitation of Co(II)(aq) on Al$_2$O$_3$. *J. Coll. Inter. Sci.* **187,** 62–82.

van den Berg C. M. G. and Nimmo M. (1987) Determination of interactions of nickel with dissolved organic material in seawater using cathodic stripping voltammetry. *Sci. Tot. Env.* **60,** 185–195.

Wilkins R. (1974) The Study of Kinetics and Mechanisms of Reactions of Transition Metal Complexes; Allyn and Bacon: Boston, MA.

Zabinsky S. I., Rehr J. J., Ankudinov A., Albers R. C., and Eller M. J. (1995) Multiple scattering calculations of X-ray absorption spectra. *Phys. Rev. B* **52,** 2995.